Could road constructions be more disastrous than an earthquake in terms of landsliding?

Hakan Tanyas[1], Tolga Gorum[2], Dalia Kirschbaum[3], and Luigi Lombardo[4]

[1]USRA/NASA
[2]Istanbul Technical University
[3]NASA Goddard Space Flight Center
[4]University of Twente

November 22, 2022

Abstract

Roads can have a significant impact on the frequency of mass wasting events in mountainous areas. However, characterizing the extent and pervasiveness of landslides over time rarely been documented due to limitations in available data sources to consistently map such events. We monitored the evolution of a road network and assessed its effect on slope stability for a ten year window in Arhavi, Turkey. The main road construction projects run in the area are associated with a hydroelectric power plant as well as other road extension works and are clearly associated with the vast majority (90.1%) of mass movements in the area. We also notice that the overall number and size of the landslides are much larger than in the naturally-occurring comparison area. This marks a strong and negative effect of human activities on the natural course of earth surface processes. Our findings show that the damage generated by the road construction is compatible with the possible effect of a theoretical earthquake with a magnitude greater than M_w=6.0. Overall, better co- and post-construction conditions should be ensured during and after road works to mitigate the risk to local communities. We also notice a significant variation in sediment transport as a result of road construction. As a result, our study fits in the big picture of Anthropocene related changes and specifically points out at problems in mountainous areas that could undoubtedly be better managed to reduce the risk to local communities.

Hosted file

supplemantary_materials.docx available at https://authorea.com/users/536491/articles/599098-could-road-constructions-be-more-disastrous-than-an-earthquake-in-terms-of-landsliding

1 **Could road constructions be more disastrous than an earthquake in terms of**

2 **landsliding?**

3 **Hakan Tanyaş[1,2], Tolga Görüm[3], Dalia Kirschbaum[1], Luigi Lombardo[4]**

4 [1]NASA Goddard Space Flight Center, Hydrological Sciences Laboratory, Greenbelt, MD, USA

5 [2]USRA, Universities Space Research Association, Columbia, MD, USA

6 [3] Istanbul Technical University, Eurasia Institute of Earth Sciences, Istanbul, Turkey

7 [4]University of Twente, Faculty of Geo-Information Science and Earth Observation (ITC),

8 Enschede, Netherlands

9 Corresponding author: Hakan Tanyaş (hakan.tanyas@nasa.gov)

10 **Key Points:**

11 - We report a distinct correlation of mass movements and major road constructions

12 - Poor engineering practices threat not only local communities but also biodiversity

13 - The impact of road construction can disturb the natural slope equilibrium to an extent
14   comparable with moderate ($> 6\,M_w$) earthquakes

15

16

Abstract

Roads can have a significant impact on the frequency of mass wasting events in mountainous areas. However, characterizing the extent and pervasiveness of landslides over time rarely been documented due to limitations in available data sources to consistently map such events. We monitored the evolution of a road network and assessed its effect on slope stability for a ten year window in Arhavi, Turkey. The main road construction projects run in the area are associated with a hydroelectric power plant as well as other road extension works and are clearly associated with the vast majority (90.1%) of mass movements in the area. We also notice that the overall number and size of the landslides are much larger than in the naturally-occurring comparison area. This marks a strong and negative effect of human activities on the natural course of earth surface processes. Our findings show that the damage generated by the road construction is compatible with the possible effect of a theoretical earthquake with a magnitude greater than $M_w=6.0$. Overall, better co- and post-construction conditions should be ensured during and after road works to mitigate the risk to local communities. We also notice a significant variation in sediment transport as a result of road construction. As a result, our study fits in the big picture of Anthropocene related changes and specifically points out at problems in mountainous areas that could undoubtedly be better managed to reduce the risk to local communities.

1 Introduction

Recent findings suggest that our planet has been going through a new geologic time, Anthropocene, in which human-driven changes dominate the Earth system and its geological records instead of natural processes (e.g., Lewis & Maslin, 2015; Steffen, Broadgate, Deutsch, Gaffney, & Ludwig, 2015). The existence of the Anthropocene is supported by the "*Great Acceleration*" graphs showing proxies of growing human activities (e.g., population, water use, transportation, etc.,) and their influence on natural systems (e.g., CO_2 emission, surface temperature, domesticated land, etc.,), which becomes quite obvious since the mid-20th century (Steffen et al., 2015; Steffen, Grinevald, Crutzen, & McNeill, 2011) and is functionally and stratigraphically distinct from the Holocene epoch (Waters et al., 2016). However, the existence of the Anthropocene still needs much evidence (Brown et al., 2013). Notably, soil erosion, as a geomorphologic process, has an essential role in the formation of the geological record. In fact, soil erosion in the Anthropocene is chiefly governed by the coupled effect of natural and human-

47 induced soil erosion processes (Poesen, 2018). In this context, we still need to better understand

48 the interactions between these processes (Brown et al., 2017).

49 In seismically active mountain ranges, landslides appear as the major erosive agent (e.g., Dadson

50 et al., 2004; Morin et al., 2018; Parker et al., 2011). Moreover, anthropogenic factors (i.e., land-

51 use change, deforestation, hill cutting, etc.,) can also be a significant contributor of landslide

52 initiations in active mountain ranges (e.g., Chang & Slaymaker, 2002; Holcombe, Beesley,

53 Vardanega, & Sorbie, 2016; Larsen & Parks, 1997; Vuillez et al., 2018). In particular, road

54 construction is reported as one of the most influential factors of landslide occurrence in

55 seismically active mountainous regions such as in India (e.g., Barnard, Owen, Sharma, & Finkel,

56 2001; Haigh, Rawat, & Bartarya, 1989), Nepal (e.g., Hearn & Shakya, 2017; McAdoo et al.,

57 2018), New Zealand (e.g., Coker & Fahey, 1993; Fransen, Phillips, & Fahey, 2001), Pakistan

58 (e.g., Atta-ur-Rahman, Khan, Collins, & Qazi, 2011; Owen et al., 2008) and Taiwan (e.g., Chang

59 & Slaymaker, 2002; Chen & Chang, 2011). This is not a surprising because hillslope cutting can

60 cause a reduction in shear strength of hill slope material and also raised or perched water tables

61 that lead to increase pore water pressure in case of rainfall event (Holcombe et al., 2016).

62 As a result, we observe an increasing number of slope failures in seismically active mountain

63 ranges such as the Himalayan region because of road construction (e.g., Froude & Petley, 2018;

64 D. N. Petley et al., 2007). However, capturing the anthropogenic effect in landslide occurrence

65 may not be a trivial task in such environments because seismicity disturbs rock masses and

66 increases landslide susceptibility irrespective of road construction (e.g., Owen et al., 2008; Tang,

67 Zhu, Qi, & Ding, 2011). Therefore, differentiating the signal of anthropogenic effect from the

68 seismic one can be a challenge in some cases. For instance, Khattak et al. (2010) and Khan et al.

69 (2013) examine the post-seismic landslide evolution following the 2015 Kashmir earthquake and

70 emphasize the possible confusion between landslides triggered by road construction and strength

71 reduction caused by seismic shaking. The same difficulty distinguishing the contribution of

72 anthropogenic and seismic factors in landslide occurrence can also be valid for slope failures that

73 occurred following the 2015 Gorkha earthquake. Jones et al. (2020) report an increased landslide

74 rate from 2016 to 2018, which is argued to be primarily associated with the increase in road-

75 construction efforts. However, the disturbance induced by the earthquake is inevitably a part of

76 the predisposing factors.

77   This implies that capturing the anthropogenic effect could be more convenient in an environment

78   at which seismicity does not play a significant role in landslide occurrence. Therefore, in this

79   study, we focus on a mountainous area located in the northeastern part of Turkey, where the site

80   has been exposed to no significant seismicity but to multiple road construction projects. We

81   examine not only expanding roads, but also mass movements associated with those roads over

82   the last 10 years. To assess the role of the anthropogenic effect, we also map landslides that do

83   not show any direct relation with roads. Ultimately, we compare our landslide inventory

84   triggered by hillslope cutting and a landslide inventory associated with an earthquake, which is

85   one of the most common triggers (D. Petley, 2012). By this comparison, we aim to better assess

86   how relevant human influence can be compared to natural processes.

87   **2 Study area**

88   The study area is located in the northeastern part of Turkey within the municipal boundaries of

89   Fındıklı, Rize, and Arhavi, Artvin. It comprises nine catchments over approximately 195 km^2

90   (Fig. 1). Volcanics and volcaniclastics are the main geological units seen in the study area

91   (MTA, 2002). Specifically, the alternation of basalt-andesitic lava, pyroclastics, sandstone, marl,

92   and clayey limestone has been observed throughout the area (Alan et al., 2019).

93   The study area extends approximately 25 km from the coastline and within the zone, elevation

94   sharply increases to 3350 m from the sea level. This reflects the steep topography in the area.

95   The maximum slope steepness within the examined area is 72º, whereas the average slope

96   steepness is 29º±11°.
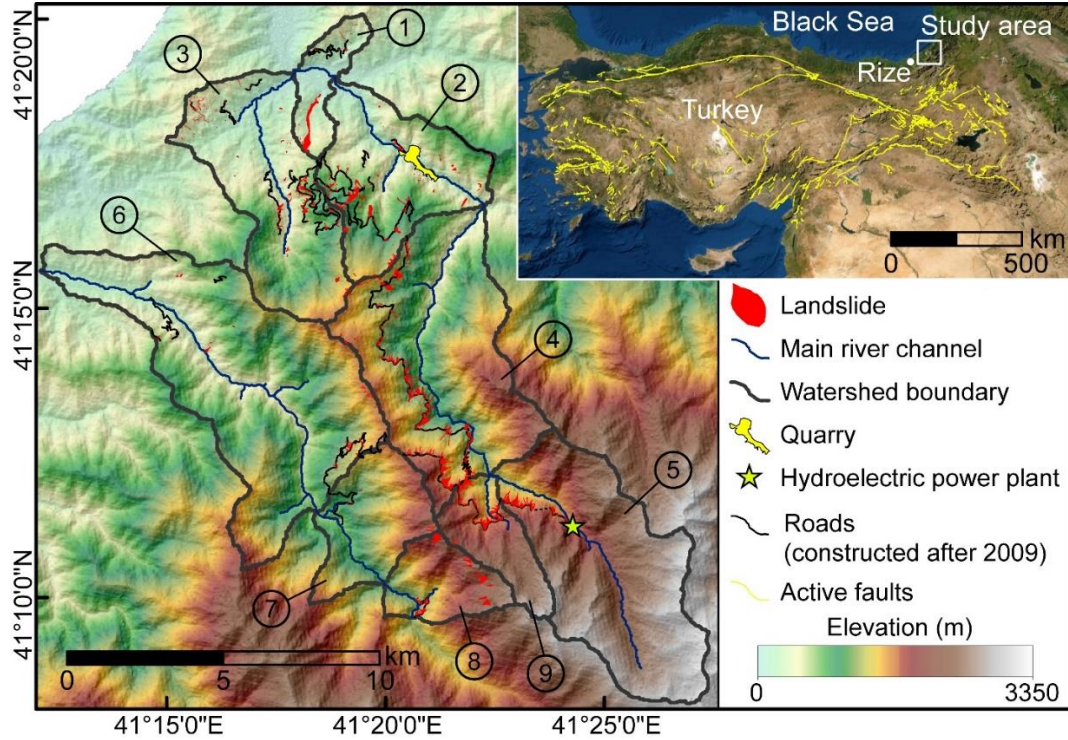
97
98 **Figure 1.** Overview of the study area. Catchments are labelled by numbers.

99 The steep topographic features of the site are coupled with a strong precipitation regime. The

100 study area is within the zone receiving the highest precipitation measured throughout Turkey

101 (Fig. 2a). Based on the 20 years (from 2000-06-01 to 2020-03-31) time series of the Integrated

102 Multi-Satellite Retrievals (IMERG) Final Run product (Huffman, Stocker, T, Nelkin, & Tan,

103 2019), which is available through Giovanni (v.4.32) (Acker and Leptoukh, 2007) online data

104 system, the average monthly precipitation of extreme events (i.e., above 0.95 quantile) is 353±40

105 mm/month. The same dataset also shows that the average daily precipitation of extreme events is

106 39±17 mm/day.

107 As for the seismicity, the study area has not been exposed to strong external forces caused by

108 earthquakes. It is approximately 270 km from the North Anatolian Fault Zone (Fig. 1). The

109 Earthquake catalog of U.S. Geological Survey (2017) shows that in the last 100 years no

110 earthquake (M_w>3) occurred within a buffer zone of 50 km radius centered within the study area

111 (Fig. 2b). The largest earthquake (M_w=6.8) occurred in 1983, approximately 120 km southeast of

112 the study area. Except for this event, only seven earthquakes of magnitude larger than 5.0 have

113 occurred in the near vicinity and the closest epicentral location is 70 km away from the study

114 area.

115
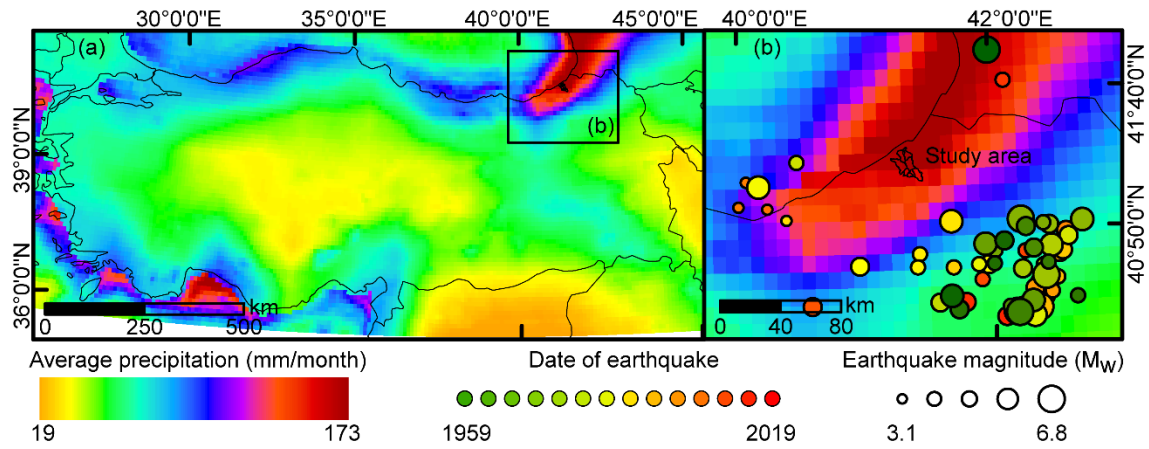
116 **Figure 2.** Maps showing the characteristics of the study area regarding (a) the precipitation
117 amounts that is the highest of entire Turkey (Huffman et al., 2019) and (b) the seismic record of
118 the area for earthquakes occurred after 1900 (U.S. Geological Survey, 2017).

119 Although the site has not been exposed to strong seismicity, landslides are one of the main
120 natural hazards threatening the East Black Sea region and extreme precipitation, land-use change
121 and road construction are the most common factors causing landslides (e.g., Nefeslioglu,
122 Gokceoglu, Sonmez, & Gorum, 2011; Raja, Çiçek, Türkoğlu, Aydin, & Kawasaki, 2017; Reis,
123 Nişanci, & Yomralioğlu, 2009). During the last decade, an increasing number of road
124 construction projects has been increasing the landslide susceptibility in the Black Sea Region
125 (e.g., Raja et al., 2017). In particular, within our study area, road constructions have a significant
126 role in landslide occurrences (Akbulut & Kurdoglu, 2015). Road construction has been
127 conducted for three main reasons: (1) to increase the accessibility to highlands to boost tourism
128 in the region (*Green Road project*, DOKAP, 2014), (2) to build a hydroelectric power plant
129 (HEPP) in the southern part of the study area and (3) to improve the road network overall. Some
130 of the roads constructed under the third category could be indirectly associated with the first two
131 classes because newly constructed roads may have further stimulated the construction of others.

132 These construction projects are met with resistance from both non-governmental environmental
133 organizations (e.g., WWF, 2020) and geoscientific community (e.g., Akbulut & Kurdoglu, 2015)
134 because the study area is within the Caucasus ecoregion, which is one of the world's 34
135 biodiversity hotspots (Şekercioğlu, Anderson, Akçay, Bilgin, et al., 2011). The Kamilet Valley
136 crossing through the study area (Sub-basins 4, 5 and 9 in Fig. 1) is one of the sites reflecting the
137 rich biodiversity of the region. It hosts numbers of endemic and rare non-endemic plants species
138 that need to be protected (Akbulut & Kurdoglu, 2015; Şekercioğlu, Anderson, Akçay, & Bilgin,

139   2011; Yuksel & Eminagaoglu, 2017). Therefore, the research question of this study -- that aims

140   at exploring the anthropogenic control on hillslope erosion processes -- also has implications on

141   the protection and sustainable development of a biodiversity hot spot.

3 Materials and method

143   We map both landslides and constructed roads from 2010 to June 2020. To create these multi-

144   temporal inventories, we use PlanetScope (3-5 m), Rapid Eye (5 m) images acquired from Planet

145   Labs (Planet Team, 2017) and high-resolution Google Earth scenes. The details of the satellite

146   images we used are presented in Table S1.

147   We create inventories based on the systematic examination of satellite images through manual

148   mapping. We always compare two images to map landslides that occurred and roads that were

149   constructed within the examined time window. We do not follow a fixed temporal resolution to

150   map landslides or roads. In fact, we aim at using all the available cloud-free satellite images.

151   Thus, the resulting temporal resolution of the landslide inventories is not fixed and actually

152   increases after 2016, following the increase in the number of available images. For instance, the

153   temporal resolution of our inventory is approximately one year between 2010 and 2011, whereas,

154   after 2016, it is much finer at up to one-month frequency (Table S1).

155   While mapping, we examine whether or not landslides are associated with road construction. For

156   this binary labelling, we manually go through the inventory and identify the ones having contact

157   with roads. If the target landslide crosses a road or is initiate right under a road cut, we label the

158   given landslide as a human-induced one.

159   Also, we group landslides that occurred and roads that were constructed based on two different

160   criteria, namely, by assigning a label describing the purpose of road construction and the

161   occurrence/construction time. For the former one, we examine the purpose of road constructions

162   and categorize them under three headings: (1) HEPP project, (2) Green Road project and (3)

163   others (i.e., roads constructed after 2010 for other reasons than Green road and HEPP projects).

164   Using the same classification, we label not only roads but also the corresponding landslides. We

165   also compare landslides associated with road constructions and the ones triggered by

166   precipitation. We do so by examining the occurrences of landslides for different catchments.

167 This allows us to better investigate the anthropogenic influence by comparing two adjacent
168 catchments exposed to different levels of external disturbances caused by road construction.

169 For the second criterion, we label landslides/roads using one year of fixed temporal windows. As
170 a result, we create 11 temporal categories that we can use to examine the evolution of both
171 landslides and roads from 2010 to June 2020 with one year temporal resolution. We do not
172 differentiate source and depositional areas of landslides and delineate them as a part of the same
173 polygon. If the existing landslides expand over time, we only map the new surface in the
174 examined time window.

175 To examine the landscape characteristics and precipitation regimes, we use Shuttle Radar
176 Topography Mission (SRTM) digital elevation models (approximately 30-m resolution) (NASA
177 JPL, 2013) and the Global Precipitation Measurement (GPM), the Integrated Multi-Satellite
178 Retrievals (IMERG) Final Run product (Huffman et al., 2019).

179 Ultimately, we compare our human-induced mass movement inventory with a sample of
180 earthquake-induced landslide inventories, available via the U.S. Geological Survey ScienceBase
181 platform (Schmitt et al., 2017; Tanyaş et al., 2017). We make this comparison to assess how
182 hazardous road construction could be compared to naturally occurring landslides. For the
183 comparison, we examine the landslides' size statistics, which has been used as a basis to identify
184 landslide-event magnitude scale (mLS) and provides a measure to quantify the severity of
185 landslide events (Malamud, Turcotte, Guzzetti, & Reichenbach, 2004). We calculate mLS using
186 the code provided by Tanyaş et al. (2018). We also calculate the slope of the power-law
187 distribution (β, power-law exponent) that the frequency-density distribution of landslides
188 exhibits (e.g., Guzzetti, Malamud, Turcotte, & Reichenbach, 2002; Malamud et al., 2004;
189 Tanyaş, van Westen, Allstadt, & Jibson, 2019) using the method proposed by Clauset et al.
190 (2009). To estimate an earthquake magnitude for an equivalent earthquake-induced landslide
191 inventory with our human-induced one, we use the empirical relation between earthquake
192 magnitude (M) and landslide-event magnitude scale (Malamud et al., 2004).

193 $mLS = 1.29 \times M - 5.65$　　　　(1)

194 **4 Results**

195 **4.1 Mapping of roads and landslides**

196 We identified the roads associated with "*HEPP*" and "*Green Road*" projects (Fig. 3a) based on
197 information from our local contacts and interviewees. They informed us about other expansion
198 work conducted along the route of the Green Road project. We could not identify the time of
199 these expansions, but we know the sections where the engineering work was carried out. We
200 labelled the roads that already exist as of January 2010 as "*Pre-2010*" based on our analyses of
201 satellite scenes. We labelled the rest of the roads constructed after 2010 as "*Others*". Based on
202 the identified roads, we also labelled corresponding mass movements (Fig. 3b).
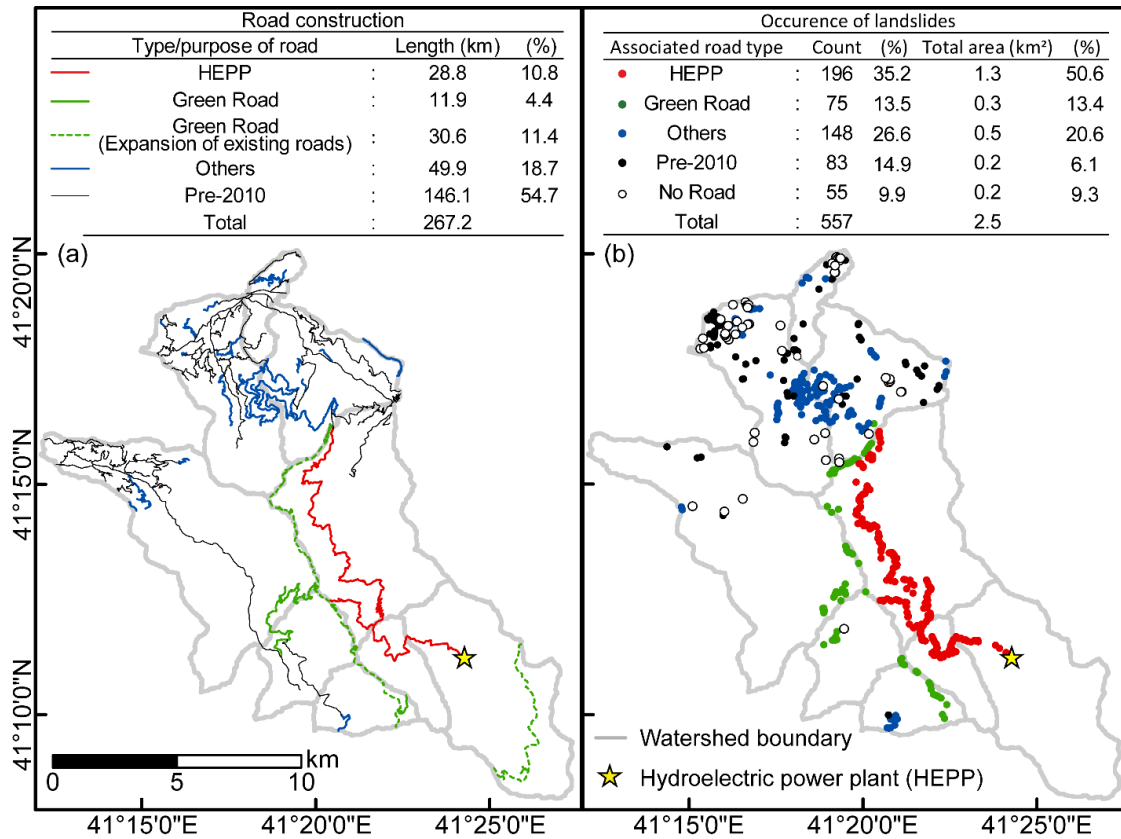
Figure 3. Maps showing the distribution of (a) the roads constructed for different purposes and
(b) the associated landslides.

206 To create these road and landslide inventories, first, we mapped both roads and landslides
207 associated with *HEPP* (Fig. 3). Mapping landslides was particularly challenging because of the
208 short-term interactions between mass movements and engineering activities. Specifically, local
209 people indicated that the excavated hillslope materials were mostly dumped into the river
210 channels during the construction, and also down the slope of the road cut. This may have also
211 induced some landslides further down the hillslope because of the additional load. Notably, this

212   makes the identification of landslides difficult because the dumped hillslope materials and
213   landslides triggered by the construction are mostly mixed and have a similar appearance in
214   satellite scenes. For instance, Figure 4 shows a segment of the road excavation conducted as part
215   of the *HEPP* project. This satellite image clearly shows that dumped materials are mixed with
216   landslides triggered by road construction. We can both see mass movements that were initiated
217   from the upper or lower hillslopes. For the former ones, we can be sure that these are human-
218   induced landslides. However, for the latter cases, we cannot differentiate whether they are solely
219   dumped materials or human-induced landslides. In fact, most likely, their genesis is the result of
220   the coupled effect of both processes.

221
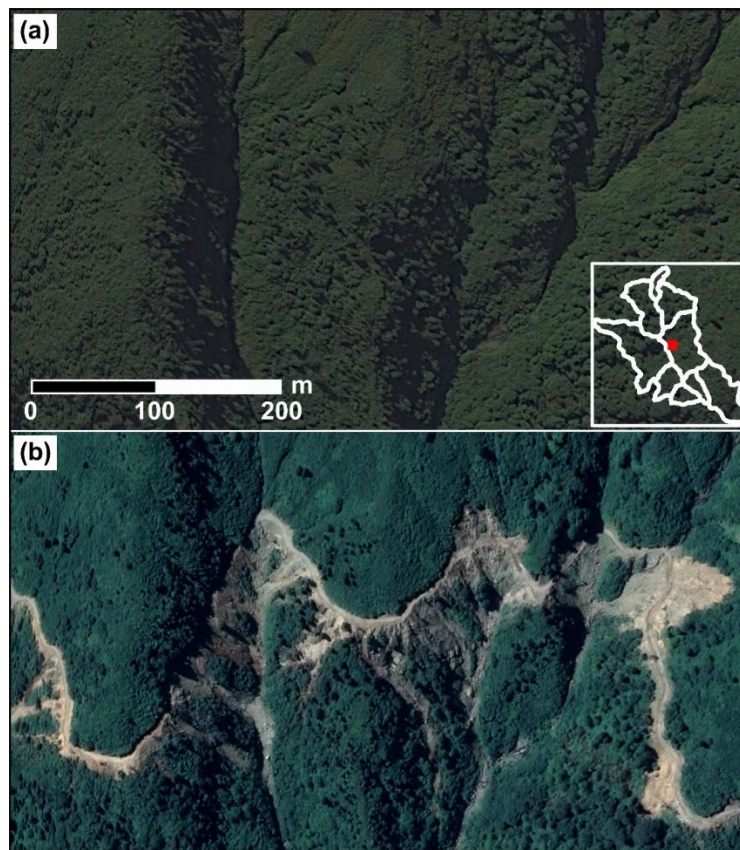
Figure 4. Satellite scenes showing the pre- and post- excavation landscape in a selected area (41°
13′ 56″ N and 41° 20′ 18″ E) along the route excavated for the *HEPP* project. The examined
segment of the road was constructed between 17th July 2016 – 6th September 2016. Within the
same period, mass movements widely occurred. We also identified some landslides enlarged
between 6th September 2016 – 9th July 2017. The location of the sample area is geographically
shown in the lower right of the panel (a).

228 Local interviews also emphasized that the road construction carried out for the *HEPP* project has
229 dramatically affected the natural course of erosional processes since 2016 (Fig. 5). They argue
230 that explosives were used in some parts of the road construction to facilitate the progress of the
231 project. This most likely weakened the shear strength of hillslope material, increasing the
232 landslide susceptibility of the given site and promoting the failures we noted.

233

234 **Figure 5.** Photos showing the mass movements on hillslopes associated with road constructions
235 of *HEPP*. The photos were taken on 15th June 2020 (Photographs courtesy of Hasan Sıtkı
236 Özkazanç).

237 Overall, the differentiation between dumped materials and human-induced landslides is
238 challenging. Regardless, these processes initiate additional anthropogenic sediment loads to
239 river channels. The local environmental organizations (*Arhavi Doğa Koruma Platformu*)
240 provided evidence to this claim in an early 2020 report where an increased sediment content was
241 noted in the Kamilet River (Fig. 6). Therefore, in this study, we did not differentiate the dumped
242 hillslope materials and landslides; instead, we considered them all as human-induced mass
243 movements.

244

245 **Figure 6.** Photos showing the intersection of Kamilet and Durguna Rivers (41º 16′ 34″ N and 41º

246 22′ 32″ E) where increased sediment content in Kamilet River caused by the *HEPP* construction

247 is evident. The pictures were taken in May 2020. Location of this spot is given in the lower right

248 of the panel (b) (Photos by Hasan Sıtkı Özkazanç).

249 We also mapped mass movements that occurred along with the Green Road project (Fig. 3).

250 Some of the mass movements occurred along existing roads, which were expanded in relation to

251 the Green Road project. Similar to the *HEPP* case, dumped hillslope materials might also play a

252 role in these mass movements. However, Figure 7 shows that the crests of some mass

253 movements extend backward from the road and therefore, we argue that these must be a mixture

254 of both dumped materials and human-induced mass movements if they are not purely human-

255 induced mass movements.

256
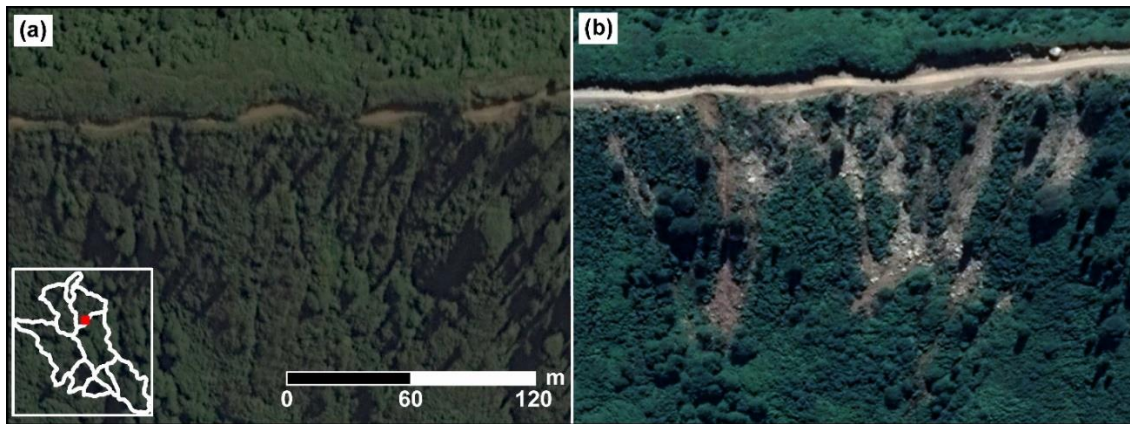
257 **Figure 7.** Google Earth scenes showing the pre- and post- expansion landscape at a selected site

258 (41º 15′ 37″ N and 41º 20′ 24″ E) along the route excavated for the Green Road project. Mass

259 movements occurred between 18th September 2017 – 27th May 2018. The location of these mass

260 movements is given in the lower left of panel (a).

261 Moreover, we mapped mass movements that occurred along other roads (i.e., *Others*) that were

262 excavated during the same period (Fig. 3). These are mostly secondary and private roads opened

263 to access agricultural sites or houses and therefore, they were created without the use of

264 explosive. Consequently, excavated materials are expected to be less compared to HEPP and

265 Green Road, which were designed for higher traffic loads that require a wider road section and

266 cut. Figure 8 shows an example of human-induced mass movements along roads labelled as

267 *Others*.

268
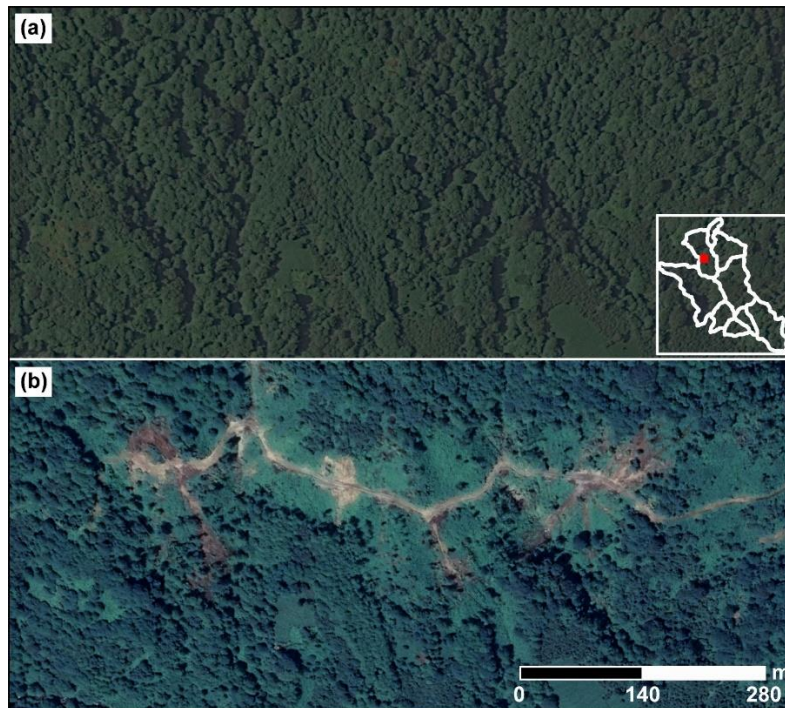
269 **Figure 8.** Google Earth scenes showing the pre- and post- road expansion conditions at a

270 selected site (41º 16′ 24″ N and 41º 17′ 51″ E) representing the mass movements categorized as

271 *Others*. The examined the segment of the road constructed between 10th September 2013 – 3rd

272 September 2014. Landslides occurred between 18th November 2017 – 27th May 2018 and 20th

273 March 2019 – 21st May 2019. The location of these mass movements is given at the lower right

274 of the panel (a).

275 Ultimately, we mapped landslides that occurred along the existing roads (*Pre-2010*) (Fig. 9) and

276 the ones triggered by natural agents irrespective of roads (*No Road*) (Fig. 10). Precipitation is the

277 most likely triggering factor for these landslides. However, for the Pre-2010 case, road works

278 should have played a crucial role in the failure mechanism by disturbing both resisting forces

279 against sliding and hydrological conditions. As for the *No Road case*, in addition to precipitation

280 as a triggering factor, some anthropogenic factors might have played a role, albeit to a much

281 lesser extent. We will elaborate on the possible contribution of those indirect anthropogenic

282 factors in Section 5.

283
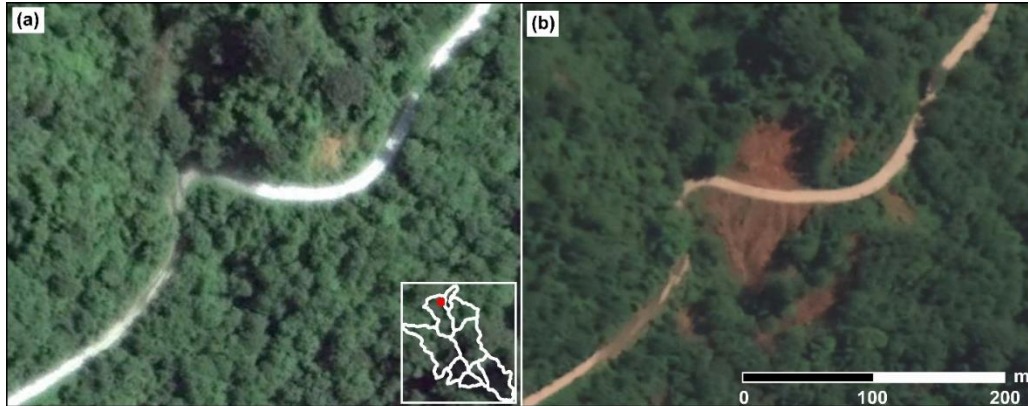
284 **Figure 9.** Google Earth scenes showing the pre- and post- landslide views at a selected site (41°

285 18′ 20″ N and 41° 20′ 14″ E), representing the mass movements that occurred along an existing

286 road (i.e., *Pre-2010*). Mass movements occurred between 3rd November 2016 – 16th April 2017.

287 The location of these mass movements is given in the lower right of the panel (a).

288

289 **Figure 10.** Google Earth scenes showing the pre- and post- landslide landscape at a selected site

290 (41° 18′ 20″ N and 41° 17′ 58″ E) representing the mass movements triggered by natural agents

14

291   (i.e., *No Road*). The landslide occurred between 17th July 2016 – 9th September 2016. The

292   location of the landslide is given in the lower left of the panel (a).

4.2 Analyses of mass movements

294   We mapped 557 mass movements and a 267.2 km long road network. Overall, 33.9% of the

295   roads were developed during the last 10 years, for various purposes (see Fig. 3a). Among them,

296   10.8% is associated with the *HEPP* project and 4.4% is related to the *Green Road* project. Also,

297   some of the existing roads have been extended in relation to the Green Road project and this

298   contribution refers to 11.4% of all roads in the study area. Moreover, 18.7% of the roads

299   constructed after 2010 are not directly associated with the *HEPP* nor the *Green Road* projects,

300   but some indirect connections could exist (*Others*).

301   We also examined mass movements in relation to road work. Our findings show that 90.1% of

302   them occurred after 2010 while being in immediate proximity to the roads (Fig. 3b). As for the

303   cumulative area of mass movements, the anthropogenic influence is also significant: 90.7% of

304   total size is associated with road constructions. Roads constructed as part of the *HEPP* project

305   has the most substantial contribution to mass movements occurrences. In the study area, 1.3 km^2

306   of mass movements were solely caused by the *HEPP* project, which refers to 50.6% of the total

307   size identified in the study area. During the last 10 years, 9.9% of landslide occurred with no

308   direct relationship with roads. In terms of total size, the influence of these landslides constitutes

309   9.3% of the total area of mass movements. This static summary is complemented below by

310   examining the variation in both road construction and landslide occurrence on a temporal basis

311   (Fig. 11 and 12). We noticed a peak value in road construction in 2012. However, the peak in the

312   constructions does not correspond to a significant number of landslides. This is mainly because

313   of the morphologic conditions encountered through the route. In fact, most of the roads we

314   mapped between 2011 and 2012 are associated with roads categorized as *Others*. The mean slope

315   steepness observed through these roads is 23º, which is lower than mean steepness encountered,

316   for instance, through the roads associated with the *HEPP* project (33º) (Fig. 12). This is also the

317   case for two other categories (i.e., *Pre-2010* and *Green Road*). They both cross relatively smooth

318   topography compared to the *HEPP* project. Specifically, the *Green Road* project mainly follows

319   the existing old road path, which passes through ridges (Fig. 3a). Therefore, a predominant part

320   of these roads did not require any hillslope cut in our study area. This explains why the mass

321 movements triggered in response to the activities of the *HEPP* project gave the largest damage

322 among different construction projects (Fig. 3b).
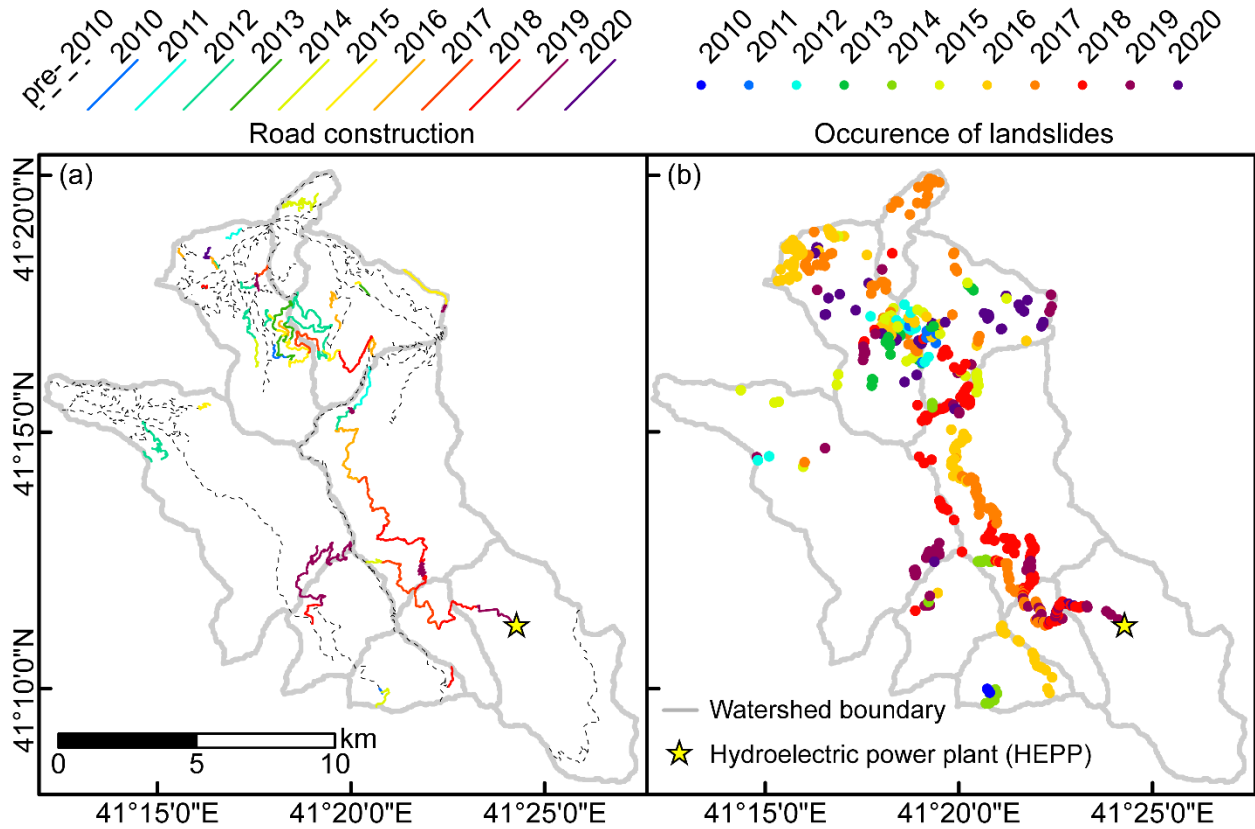
Figure 11. Maps showing the temporal evolution of (a) the roads and (b) the associated landslides.

326 After 2016, the total length of constructed roads per year increases (see, Fig. 12a). As a result,

327 the number of landslides associated with road construction also significantly increases after

328 2016. Since then, the contribution of naturally triggered landslides becomes negligible (Fig.

329 12b).

330 In 2016, an increase in the landsliding trend could also be linked to strong precipitation (average

331 monthly precipitation was approximately 200 mm/month in 2016). However, in the following

332 years, landslide rates are still higher than pre-2016 levels, although the amount of precipitation is

333 equal or less then the pre-2016 levels (<150 mm/month). These findings indicate that the

334 increase in landslide rate is mostly due to road constructions regardless of extreme rainfall
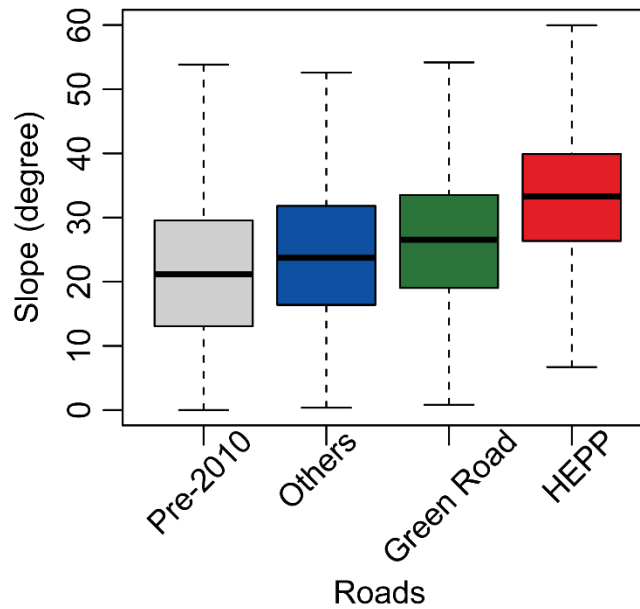
335 events.

336

337
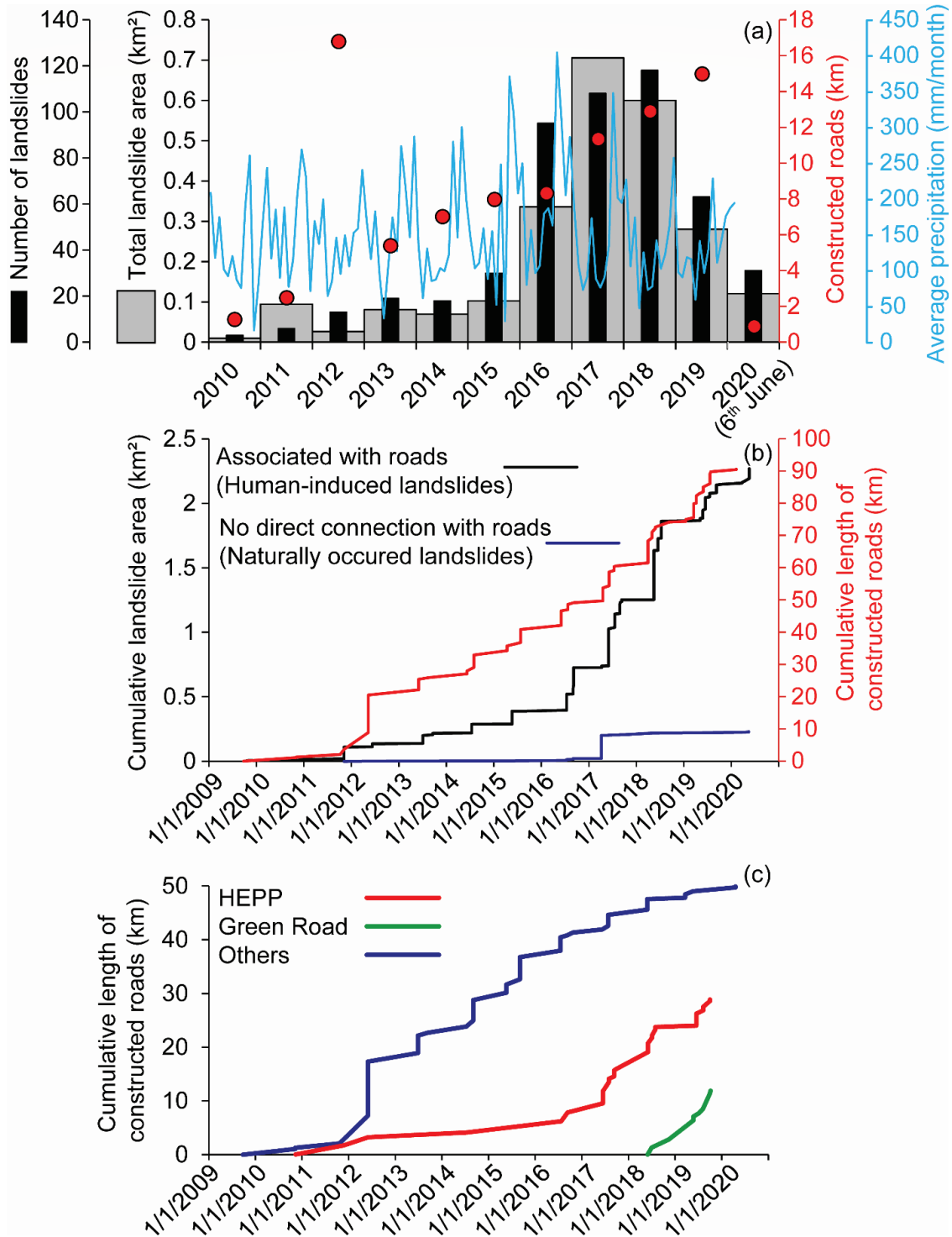
Figure 12. Plots showing the yearly variation in road constructions and landslide occurrences from 2010 to 2020. (a) The number and the total area of landslides against the entire length of

340 constructed roads. (b) The cumulative trend in total landslide size and road length and (c) the

341 roads constructed for different purposes.

342

343 **Figure 13.** Boxplots showing the range of slope steepness along roads constructed for different

344 purposes.

345 We also examined how the road constructions evolved after 2010 in each catchment and,

346 consequently, how this affected the occurrences of mass movements per hydrological unit.

347 Figure 14 shows the summary of this temporal evolutions. For this analysis, we excluded the

348 naturally occurring landslides. Our findings show that if there is no significant road construction,

349 the number of mass movements is relatively low. For instance, catchments 1, 2, 3 and 4 are

350 adjacent catchments. Among them, catchment 1 is the only hydrological unit where the total

351 length of constructed roads in the last 10 years is less than 5 km. The associated total landslide

352 size in catchment 1 is 0.02 km^2, whereas, in the three other catchments (2,3 and 4), it ranges

353 from 0.24 km^2 to 0.82 km^2. We observed a similar situation in catchments 5, 8 and 9, where we

354 identified a relatively low amount of road constructions (<~5 km) associated with a limited

355 number of landslides (Fig. 14). In catchments 6 and 7, the total length of the road (~10 km) is in

356 between two other sets we mentioned above, but we identified 28 and 9 landslides in these

357 catchments. These roads are mostly associated with the *Green Road* project and thus the limited

358 number of landslides is most likely because of the steepness of the route followed during the

359 construction (Fig. 13).

360

361
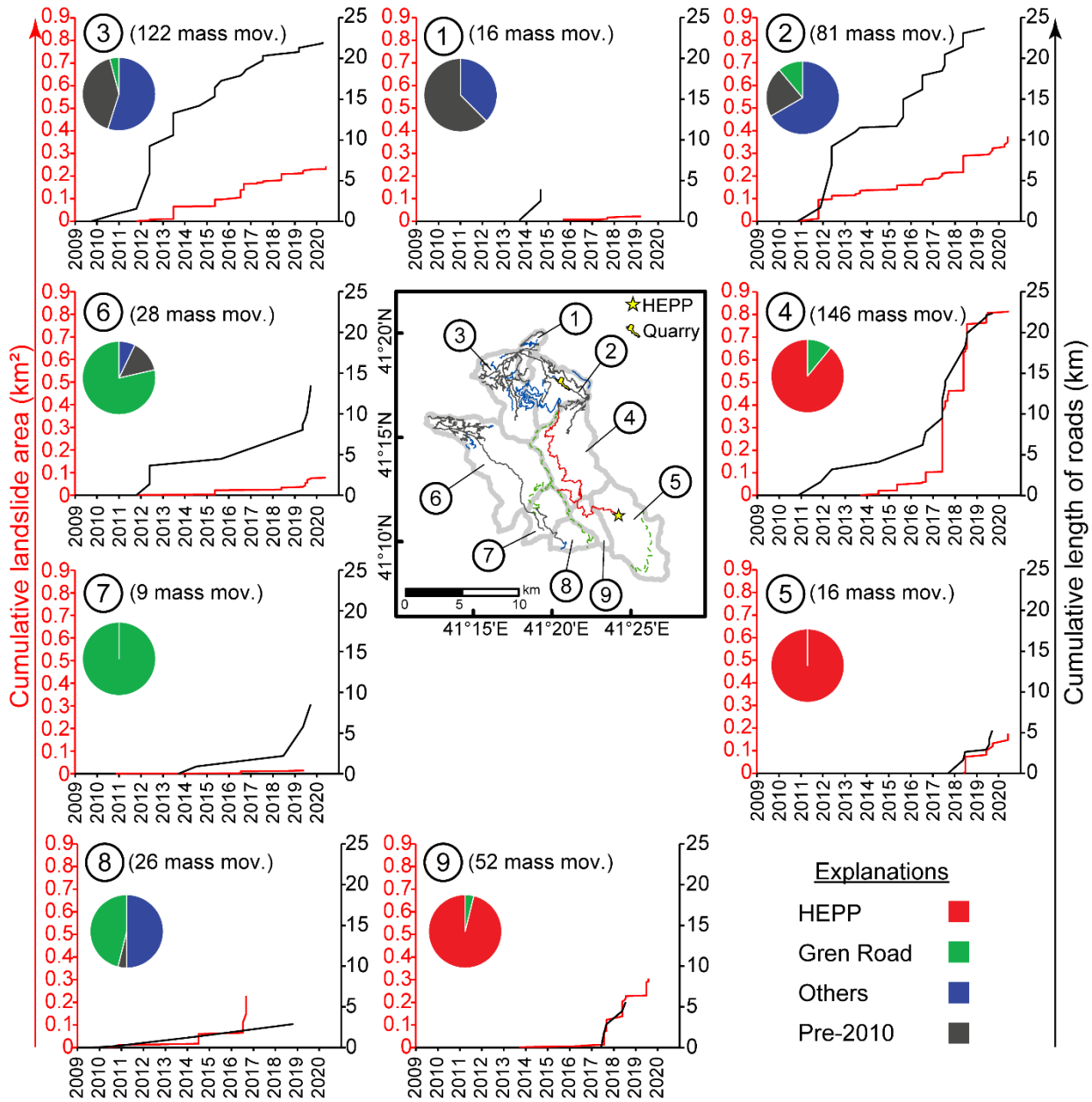
Figure 14. Figure showing the temporal evolution of both roads and landslides within each catchment from 2010 to June 2020. Catchments 2, 3 and 4 appear as hydrological units exposed to the highest road construction and consequently, the largest number of mass movements.

We also compared human-induced landslides with naturally occurred ones in terms of slope steepness and size of landslides. Figure 15 shows that slope steepness of human-induced landslides varies quite broadly compared to naturally occurred landslides. Hillslopes where the

368   slope steepness ranges from 15º to 50º are associated with a minimum of 20 and a maximum of

369   100 human-induced landslides. Conversely, the frequency of naturally occurring landslides

370   increases up to 30º (with a minimum of five and a maximum of 15 landslides), and then sharply

371   decreases for steeper slopes. This large difference is undoubtedly induced by road excavations

372   performed on steep slopes, as demonstrated by the much more numerous mass movements that

373   occurred under anthropic disturbance. In fact, the same slope ranges appear to be mostly stable

374   under natural conditions. Also, there is a large difference in average landslide size triggered by

375   road constructions and natural agents. The average size of human-induced landslides is

376   approximately ~20,000 m^2 in the steepest slopes (i.e., 55º-60º), whereas the maximum average

377   size of naturally occurring landslides is ~1000 m^2.
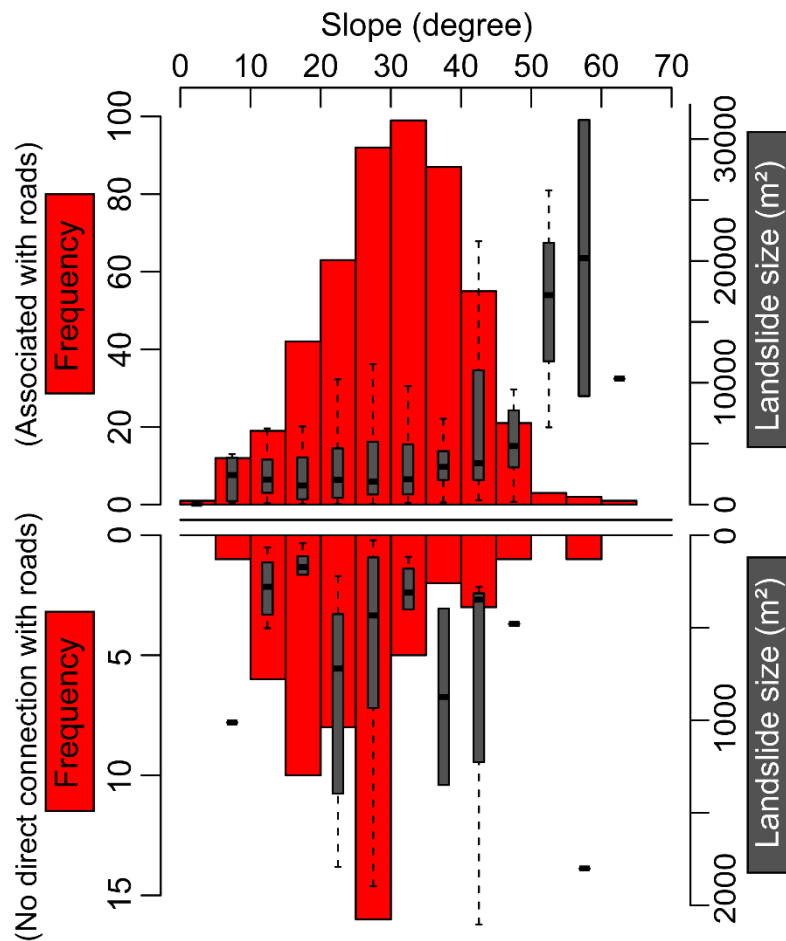
378

379   **Figure 15.** The comparison of human-induced landslides (top panel) with naturally occurred

380   (bottom panel) ones in terms of slope steepness and landslide size characteristics.

381   **5 Discussion**

382   In this study, we provide quantitative, thorough systematically mapping mass movement rate
383   after major road constructions in a mountainous region that is exposed to strong precipitation
384   regimes.   We specifically chose this region because seismicity does not play an active role here
385   and therefore, capturing the anthropogenic effect on slope stability is more evident than in
386   tectonically active mountainous regions such as Nepal, India or Pakistan. In tectonically active
387   areas, the legacy of previous earthquakes could last for a long period, increasing the landslide
388   susceptibility (R. N. Parker et al., 2015). In particular, after strong earthquakes, the elevated
389   susceptibility is noticeable in the following years (up to nine years) and it decreases over time
390   (e.g., Fan et al., 2018). Consequently, in such environments, it would be challenging to
391   decompose the signal of earthquake legacy from anthropic disturbances. Precipitation could also
392   add another layer of complexity. In fact, the occurrence of a landslide or a population of
393   landslides is always controlled by multiple predisposing and triggering factors (e.g., geotechnical
394   properties, hydrologic conditions, land cover, external loads, etc.,) (e.g., Jaboyedoff et al., 2018).
395   Capturing the relative contribution of each conditional factor requires not only highly detailed
396   temporal landslide inventories -- where we can assess the exact date of occurrence of each
397   landslide -- but also quantitative measurements of the predisposing factors at a given time.
398   Notably, we lack such detailed datasets in this paper, and this is often the case in many landslide
399   susceptibility studies, even when multi-temporal models are built (e.g., Guzzetti et al., 2005).

400   Despite the complexity we faced and the limited temporal information on other controlling
401   factors, we could still investigate whether a relationship exists between slope failures and
402   anthropogenic effect. To address this issue, we made a binary classification distinguishing
403   human-induced and naturally occurring landslides on the basis of satellite images. However, in
404   some cases, this identification was challenging, as well. For instance, the largest landslide we
405   mapped within the region occurred on 7th November 2016, following a strong precipitation event
406   (Ersoy, 2017). This event was a shallow earth-slide flow that affected an area of approximately
407   0.2 km^2 within the Kireçli village (Fig. 16). Satellite images show that the crest of the landslides
408   is precisely aligned with an existing road. Some parts of the road failed as a result of this
409   landslide (Ersoy, 2017). The complexity in the interpretation arose because this landslide could
410   also be linked to natural landscape evolution processes. In fact, the landslide initiated at the ridge
411   of the slope where the susceptibility is generally higher. Thus, the shallow landslide might have
412   been triggered regardless of the possible influence of the road.

413 In such cases, we labelled landslides as naturally occurring ones since we do not have adequate
414 support to argue that they are human-induced. We did this to implement a conservative approach
415 in our analyses. However, emphasis should still be given to the possible direct or indirect
416 anthropogenic effects. In fact, the road could have a direct implication by increasing the pore
417 water pressure at the crest of the landslide. Also, the external loads associated with traffic might
418 be another likely contributor to the landslide initiation. This event is a very interesting example
419 also because of the existence of an active rock quarry approximately 3 km east. There, to dig into
420 the slope and collect the material explosives are commonly used. Our local contacts informed us
421 that some damages had been observed at houses in villages close to the quarry (i.e., Dikyamaç,
422 Güneşli, Dereüstü villages). Among them, the Dereüstü village is located approximately 2.5 km
423 northwest of the quarry, at a comparable distance to the mudflow location. Therefore, the
424 disturbance exerted by activities related to the quarry might have also played a role in triggering
425 the landslide mentioned above.

426
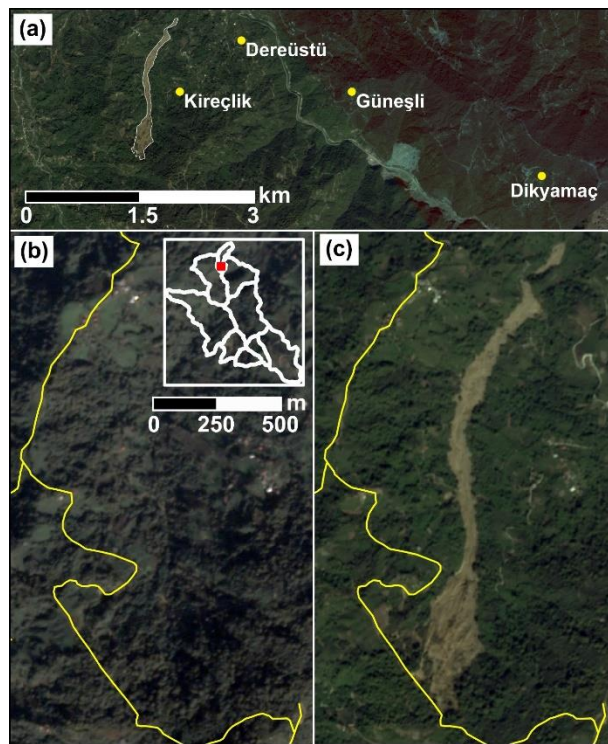
427 **Figure 16.** PlanetScope scenes showing the pre- and post- landslide landscape of the largest
428 landslide mapped within the study area (41º 17′ 37″ N and 41º 18′ 27″ E). This landslide
429 occurred on 7th November 2016. The location with respect to our study area is given in the upper
430 right of the panel (b). Yellow lines in the panel (b) and (c) indicate roads.

431   A similar anthropogenic effect, if not even stronger, could also be valid for landslides triggered
432   along the roads constructed as part of the *HEPP* project, because of the explosives directly used
433   to cut the hillslope. In fact, apart from hillslope cuts, explosives have been used in the last
434   segment of the road approaching the *HEPP* site. In this section, approximately 620 m of the
435   route passes through a tunnel. In such steep terrain, any time a new road is constructed, the
436   damage to the slope is almost inevitable unless extreme precautions are taken. This is also
437   reported in the literature. For instance, Froude and Petley (2018) report that from 2004 to 2016,
438   30% and 43% of fatal landslides occurred in India and Nepal are associated with road
439   constructions. In these cases, the high landslide rates are not due to the lack of engineering
440   solutions. In fact, landslides triggered in response to road construction projects are a well-known
441   issue for both India and Nepal. The required and appropriate engineering practices necessary to
442   minimize environmental damage have already been documented (e.g., Hearn and Shakya, 2017).
443   The observed landslide hazard associated with road construction is mostly due to neglected
444   engineering solutions (Hearn & Shakya, 2017). Therefore, road construction in mountainous
445   regions should not be envisioned unless the required investment in road design is available
446   (Hearn & Shakya, 2017; Valdiya, 2014). Notably, the site we examined is a good example where
447   road construction has widely damaged the landscape, and it is clear that better precaution or
448   stabilization investments should have been put into practice.

449   To assess the consequences of human effects on mass movements, we also compared our
450   landslide inventory (i.e., only the landslides associated with road constructions) with nine
451   earthquake-induced landslide-event inventories sharing similar landslide-event magnitude and
452   total landslide area. Figure 17 shows that the human-induced mass movement inventory we
453   mapped is compatible with landslide-events triggered by earthquakes having magnitudes varying
454   from $M_w=5.9$ to $M_w=7.2$. This observation is made regardless of climatic and morphologic
455   conditions.
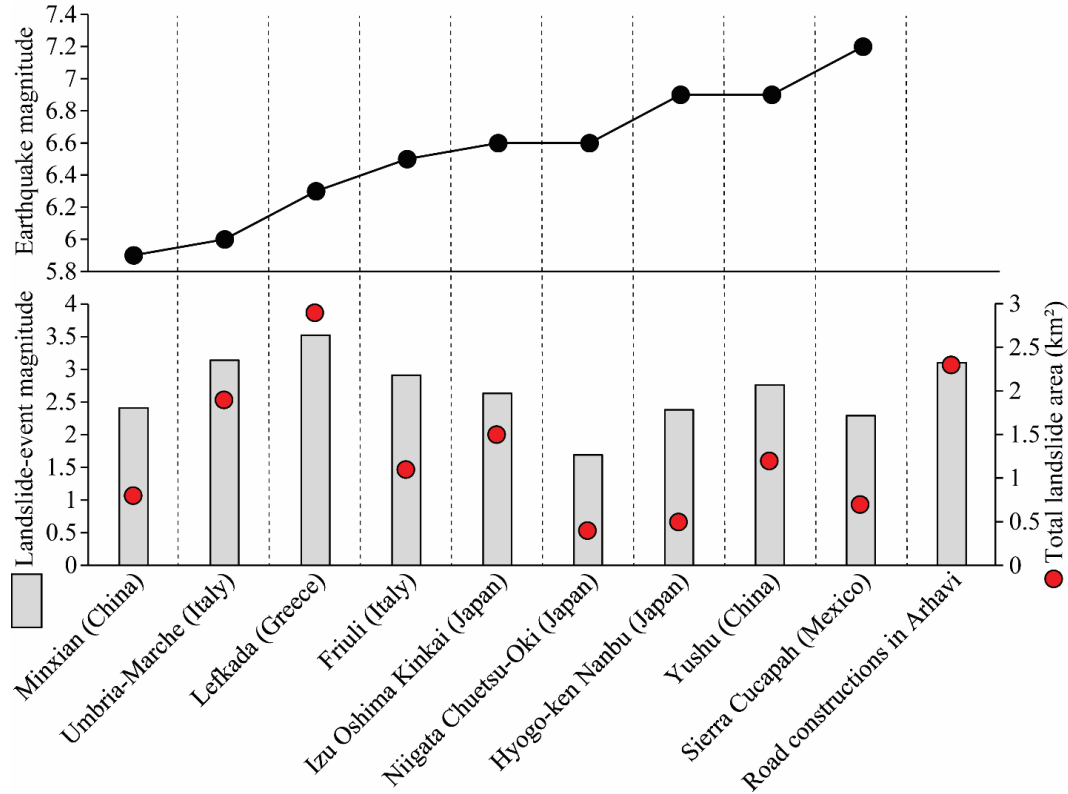
Figure 17. Comparison between our human-induced mass movement inventory and nine earthquake-induced landslide inventories. Landslide-event magnitudes were calculated based on Tanyaş et al. (2018).

Among the ten examined cases, the total surface affected by landslides changes significantly from one case to another, with many cases showing a much larger spatial extent compared to our study site. Therefore, for a better comparison, we further investigated the landslide inventory associated with the 2013 Minxian earthquake (M_s=6.6 based on the China Earthquake Network Center and M_w=5.9, according to USGS), where the extent of the region affected by landslides is equivalent to our study area. Specifically, the earthquake occurred between Minxian and Zhangixan (in the Gansu Province, China) on a thrust fault and triggered 2330 co-seismic landslides covering ~200 km^2 (Xu, Xu, Shyu, Zheng, & Min, 2014), which is also compatible with our study area where the examined catchments cover approximately 195 km^2.

The cumulated extent of all the landslide polygons associated with the Minxian earthquake is 0.8 km^2, whereas the total size of our human-induced landslides is 2.3 km^2. This shows that even the mass movements solely related to the *HEPP* project (total landslide area is 1.3 km^2) can significantly surpass the total co-seismic landslide size induced by the Minxian earthquake.

473   Before comparing the two inventories in terms of their size statistics, we first analyzed in terms

474   of climatic and morphologic conditions. To collate the climatic information, we used the 20

475   years (from 2000-06-01 to 2020-03-31) precipitation time series accessed via the IMERG Final

476   Run product, for both sites. Figure 18a shows that both sites have similar precipitation regimes,

477   although the precipitation is relatively higher in our study area. Also, slope and local relief

478   (derived from the SRTM DEM at ~30m) observed in our study area indicate rougher terrain

479   within the landslide-affected area compared to those affected by the Minxian earthquake (Fig.

480   18b and 18c).

481   We recognize that the two different sites cannot be thoroughly compared because a much more

482   thorough assessment should be made accounting for detailed

483   geological/geotechnical/hydrological data. However, on the basis of the simplified overview we

484   provide, we can hypothesize that if an earthquake with comparable magnitude to Minxian would

485   occur in our study area, the resultant landslide event should be more significant because our

486   study area is associated with higher precipitation and steeper terrain conditions.

487
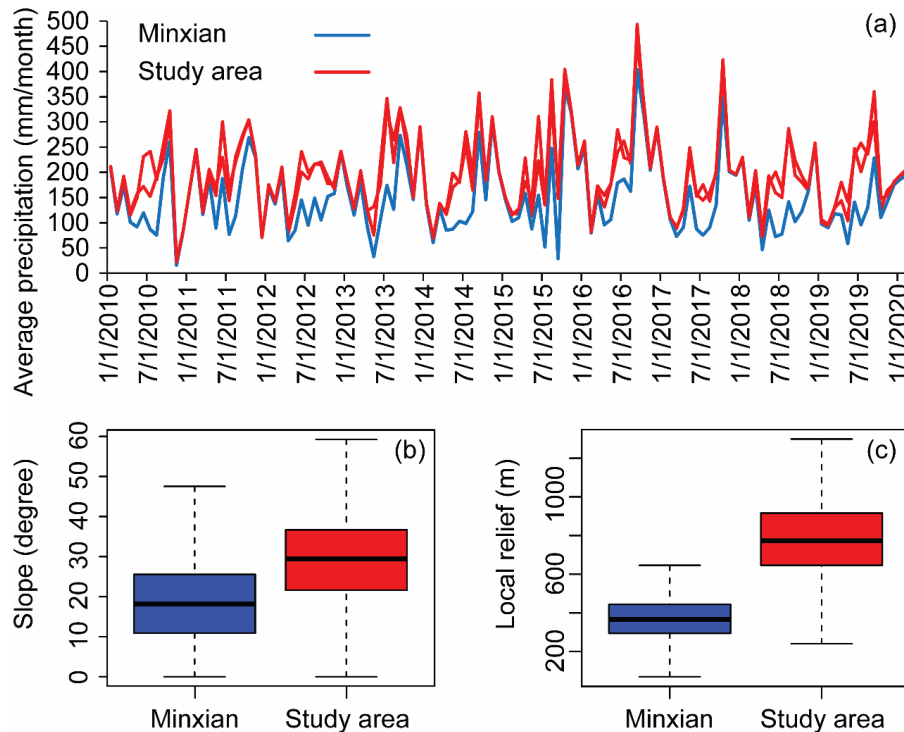
488   **Figure 18.** Plots comparing our study area with the landslide affected area of 2013 Minxian

489   earthquake regarding (a) precipitation amounts, (b) slope steepness and (c) local relief.

25

490   The comparison between the frequency-density distributions of the human-induced landslides we

491   mapped and those naturally triggered by the 2013 Minxian earthquake shows that larger

492   landslides were triggered in our Turkish site (Fig. 19). The power-law exponents calculated for

493   both our inventory (β=-2.7) and the Minxian inventory (β=-2.3) are close to each other and align

494   well with distributions documented in the literature. In fact, power-law exponents of naturally

495   occurred landslide inventories fall in the range 1.4–3.4, with a central tendency 2.3–2.5 (Stark &

496   Guzzetti, 2009; Tanyaş et al., 2018; Van Den Eeckhaut, Poesen, Govers, Verstraeten, &

497   Demoulin, 2007).

498   We also calculated the landslide-event magnitudes of our human-induced landslide inventory

499   (mLS=3.1) and the Minxian inventory (mLS=2.4). The difference between the two cases are

500   consistent with our initial assumption that if a similar earthquake occurred in our study area, it

501   would be more disastrous. In fact, based on the empirical relation between earthquake magnitude

502   (M) and landslide-event magnitude scale proposed by Malamud et al. (2004), the earthquake

503   magnitude for an equivalent earthquake-induced landslide inventory would be 6.8. This shows

504   how destructive the anthropogenic effect on geomorphological processes could be compared to

505   natural processes. The destruction produced by the road constructions conducted in the last 10

506   years is compatible with the possible effect of a theoretical earthquake with a magnitude greater

507   than 6.0.

508
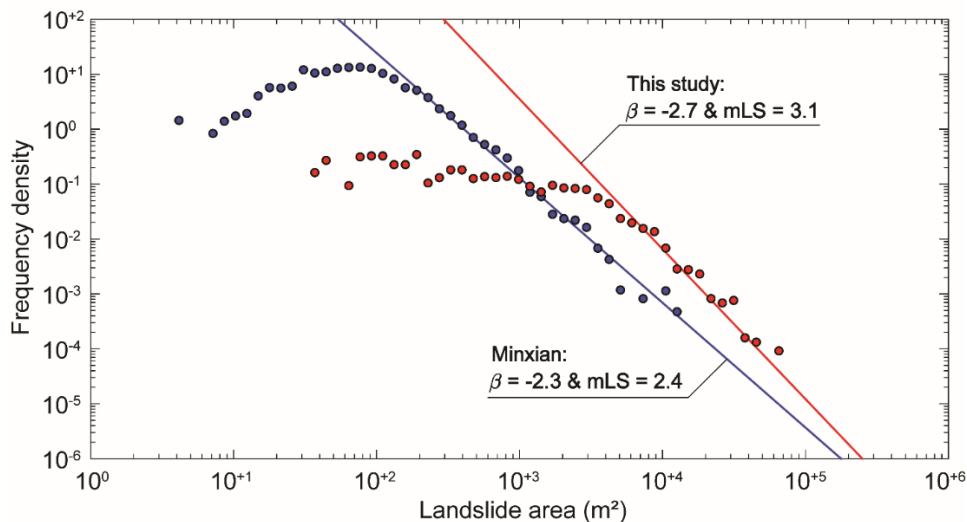
509   **Figure 19.** Frequency-density curves plotted for the landslides associated with roads in our study

510   area (red) and landslide triggered by the 2013 Minxian earthquake (blue). Power-law exponents

511 (β) were calculated based on the method proposed by Clauset et al. (2009), whereas power-law

512 fits and landslide-event magnitudes were identified based on Tanyaş et al. (2018).

6 Conclusions

514 In this study, we report a distinct correlation of mass movements and major road constructions

515 that explicitly shows human impact on mountainous environments which are under

516 anthropogenic disturbance recently. Our results further suggest that slope instabilities increased

517 drastically after major service road constructions for hydroelectric power plants and as well as

518 other road extension works. Despite the high precipitation amounts in the region, naturally

519 occurring landslides represent a minor percentage both in number and landslide-size-

520 characteristics when compared to the equivalent human-induced mass movements. Regardless of

521 the natural hillslope processes at play, the poor implementation of engineering practices able to

522 ensure stable slope conditions in co- and post- construction phases not only resulted in dangerous

523 widespread landslides but also caused a substantial change in the sediment transport along with

524 the river network. We could not access enough information on the potential effects of this to

525 quantify increases in sediment loads. However, in the long term, the coarse nature of the material

526 removed from the slopes could also clog narrow river passages, potentially damming small

527 sections of the river network. This could further induce a chain of disastrous events, which could

528 affect not only people living nearby but also the rich biodiversity of the region that needs to be

529 protected. This actually means that all endemic-rare plant and animal species exist in Kamilet

530 Valley are in danger now because of the poor engineering practice. Our results emphasize the

531 need to consider erosion and post changes in hillslope processes and sediment flux that further

532 lead to additional threats to the local community and biodiversity in response to poor engineering

533 practices any other anthropogenic disturbances.

534 We also stress that the impact of road construction can disturb the natural slope equilibrium to an

535 extent comparable with moderate (larger than 6 M_w) earthquakes. Such an observation implies

536 that human activities can have a large, if not even dominant, impact on landscape evolution and

537 the natural regime of surface processes. This is part of the definition of Anthropocene, an age

538 where our society shapes nature for our purposes, frequently at the risk of damaging ourselves.

References

547 Akbulut, S., & Kurdoglu, O. (2015). Türkiye'de acil ve öncelikle korunmasi gereken bir alan:

548   Kamilet ve Durguna Vadileri (Arhavi) ve koruma gerekçeleri. *Kastamonu Üniversitesi*

549   *Orman Fakültesi Dergisi*, *15*(2), 279-296 (in Turkish).

550 Alan, I., Balci, V., Keskin, H., Altun, I., Boke, N., Demirbag, H., … Hanilci, N. (2019).

551   Tectonostratigraphic characteristics of the area between Çayeli (Rize) and Ispir (Erzurum).

552   *Maden Tetkik ve Arama Dergisi*, *158*(158), 1–29.

553 Atta-ur-Rahman, Khan, A. N., Collins, A. E., & Qazi, F. (2011). Causes and extent of

554   environmental impacts of landslide hazard in the Himalayan region: a case study of Murree,

555   Pakistan. *Natural Hazards*, *57*(2), 413–434. https://doi.org/10.1007/s11069-010-9621-7

556 Barnard, P. L., Owen, L. A., Sharma, M. C., & Finkel, R. C. (2001). Natural and human-induced

557   landsliding in the Garhwal Himalaya of northern India. *Geomorphology*, *40*(1), 21–35.

558   https://doi.org/https://doi.org/10.1016/S0169-555X(01)00035-6

559 Brown, A. G., Tooth, S., Bullard, J. E., Thomas, D. S. G., Chiverrell, R. C., Plater, A. J., …

560   Aalto, R. (2017). The geomorphology of the Anthropocene: emergence, status and

561   implications. *Earth Surface Processes and Landforms*, *42*(1), 71–90.

562   https://doi.org/10.1002/esp.3943

563 Brown, A. G., Tooth, S., Chiverrell, R. C., Rose, J., Thomas, D. S. G., Wainwright, J., …

564   Downs, P. (2013). The Anthropocene: is there a geomorphological case? *Earth Surface*

565   *Processes and Landforms*, *38*(4), 431–434. https://doi.org/10.1002/esp.3368

566 Chang, J., & Slaymaker, O. (2002). Frequency and spatial distribution of landslides in a

567   mountainous drainage basin: Western Foothills, Taiwan. *CATENA*, *46*(4), 285–307.

568   https://doi.org/https://doi.org/10.1016/S0341-8162(01)00157-6

569   Chen, Y.-J., & Chang, K.-C. (2011). A spatial–temporal analysis of impacts from human

570   development on the Shih-men Reservoir watershed, Taiwan. *International Journal of*

571   *Remote Sensing*, *32*(24), 9473–9496. https://doi.org/10.1080/01431161.2011.562253

572   Clauset, A., Shalizi, C. R., & Newman, M. E. J. (2009). Power-law distributions in empirical

573   data. *SIAM Review*, *51*(4), 661–703. https://doi.org/10.1137/070710111

574   Coker, R. J., & Fahey, B. D. (1993). Road-related mass movement in weathered granite, Golden

575   Downs and Motueka Forests, New Zealand: a note. *Journal of Hydrology (New Zealand)*,

576   *31*(1), 65–69. Retrieved from http://www.jstor.org/stable/43944699

577   Dadson, S. J., Hovius, N., Chen, H., Dade, W. B., Lin, J.-C., Hsu, M.-L., … Stark, C. P. (2004).

578   Earthquake-triggered increase in sediment delivery from an active mountain belt. *Geology*,

579   *32*(8), 733–736. https://doi.org/10.1130/G20639.1

580   DOKAP. (2014). *Doğu Karadeniz Projesi (DOKAP) Eylem Planı (2014-2018)*.

581   Ersoy, S. (2017). *2016 Yılı Doğa Kaynaklı Afetler Yıllığı "Dünya ve Türkiye."* Jeoloji

582   Mühendisleri Odası Yayınları No: 129, Ankara (in Turkish).

583   Fan, X., Domènech, G., Scaringi, G., Huang, R., Xu, Q., Hales, T. C., … Francis, O. (2018).

584   Spatio-temporal evolution of mass wasting after the 2008 Mw 7.9 Wenchuan earthquake

585   revealed by a detailed multi-temporal inventory. *Landslides*, *15*(12), 2325–2341.

586   https://doi.org/10.1007/s10346-018-1054-5

587   Fransen, P. J. B., Phillips, C. J., & Fahey, B. D. (2001). Forest road erosion in New Zealand:

588   overview. *Earth Surface Processes and Landforms*, *26*(2), 165–174.

589   https://doi.org/10.1002/1096-9837(200102)26:2<165::AID-ESP170>3.0.CO;2-#

590   Froude, M. J., & Petley, D. N. (2018). Global fatal landslide occurrence from 2004 to 2016.

591   *Natural Hazards and Earth System Sciences*, *18*(8), 2161–2181.

592   https://doi.org/10.5194/nhess-18-2161-2018

593   Guzzetti, F., Malamud, B. D., Turcotte, D. L., & Reichenbach, P. (2002). Power-law correlations

594   of landslide areas in central Italy. *Earth and Planetary Science Letters*, *195*(3–4), 169–183.

595   https://doi.org/10.1016/S0012-821X(01)00589-1

596 Haigh, M. J., Rawat, J. S., & Bartarya, S. K. (1989). Environmental Indicators of Landslide
597   Activity along the Kilbury Road, Nainital, Kumaun Lesser Himalaya. *Mountain Research*
598   *and Development*, *9*(1), 25–33. https://doi.org/10.2307/3673462

599 Hearn, G. J., & Shakya, N. M. (2017). Engineering challenges for sustainable road access in the
600   Himalayas. *Quarterly Journal of Engineering Geology and Hydrogeology*, *50*(1), 69–80.
601   https://doi.org/10.1144/qjegh2016-109

602 Holcombe, E. A., Beesley, M. E. W., Vardanega, P. J., & Sorbie, R. (2016). Urbanisation and
603   landslides: hazard drivers and better practices. *Proceedings of the Institution of Civil*
604   *Engineers - Civil Engineering*, *169*(3), 137–144. https://doi.org/10.1680/jcien.15.00044

605 Huffman, G., Stocker, E. F., T, B. D., Nelkin, E. J., & Tan, J. (2019). GPM IMERG Final
606   Precipitation L3 1 day 0.1 degree x 0.1 degree V06. *Edited by Andrey Savtchenko,*
607   *Greenbelt, MD, Goddard Earth Sciences Data and Information Services Center (GES*
608   *DISC).*

609 Jaboyedoff, M., Michoud, C., Derron, M. H., Voumard, J., Leibundgut, G., Sudmeier-Rieux, K.,
610   … Leroi, E. (2018). Human-induced landslides: Toward the analysis of anthropogenic
611   changes of the slope environment. *Landslides and Engineered Slopes. Experience, Theory*
612   *and Practice; CRC Press: Boca Raton, FL, USA*, 217–232.

613 Jones, J., Boulton, S., Bennett, G., Whitworth, M., & Stokes, M. (2020). Himalaya mass-
614   wasting: impacts of the monsoon, extreme tectonic and climatic forcing, and road
615   construction. *EGU General Assembly 2020*.
616   https://doi.org/https://doi.org/10.5194/egusphere-egu2020-8702

617 Khan, S. F., Kamp, U., & Owen, L. A. (2013). Documenting five years of landsliding after the
618   2005 Kashmir earthquake, using repeat photography. *Geomorphology*, *197*, 45–55.
619   https://doi.org/10.1016/j.geomorph.2013.04.033

620 Khattak, G. A., Owen, L. A., Kamp, U., & Harp, E. L. (2010). Evolution of earthquake-triggered
621   landslides in the Kashmir Himalaya, northern Pakistan. *Geomorphology*, *115*(1–2), 102–
622   108. https://doi.org/10.1016/j.geomorph.2009.09.035

623 Larsen, M. C., & Parks, J. E. (1997). How wide is a road? The association of roads and mass-
624   wasting in a forested montane environment. *Earth Surface Processes and Landforms: The*
625   *Journal of the British Geomorphological Group*, *22*(9), 835–848.

626 Lewis, S. L., & Maslin, M. A. (2015). Defining the Anthropocene. *Nature*, *519*, 171+.

627 Malamud, B. D., Turcotte, D. L., Guzzetti, F., & Reichenbach, P. (2004). Landslide inventories
628   and their statistical properties. *Earth Surface Processes and Landforms*, *29*(6), 687–711.
629   https://doi.org/10.1002/esp.1064

630 McAdoo, B. G., Quak, M., Gnyawali, K. R., Adhikari, B. R., Devkota, S., Rajbhandari, P. L., &
631   Sudmeier-Rieux, K. (2018). Roads and landslides in Nepal: how development affects
632   environmental risk. *Natural Hazards and Earth System Sciences*, *18*(12), 3203–3210.
633   https://doi.org/10.5194/nhess-18-3203-2018

634 Morin, G. P., Lavé, J., France-Lanord, C., Rigaudier, T., Gajurel, A. P., & Sinha, R. (2018).
635   Annual Sediment Transport Dynamics in the Narayani Basin, Central Nepal: Assessing the
636   Impacts of Erosion Processes in the Annual Sediment Budget. *Journal of Geophysical*
637   *Research: Earth Surface*, *123*(10), 2341–2376. https://doi.org/10.1029/2017JF004460

638 MTA. (2002). 1:500 000–scale map of Turkey. *General Directorate of Mineral Research and*
639   *Exploration (MTA), Ankara, Turkey*.

640 NASA JPL. (2013). NASA Shuttle Radar Topography Mission United States 1 Arc Second.
641   NASA EOSDIS Land Processes DAAC, USGS Earth Resources Observation and Science
642   (EROS) Center, Sioux Falls, South Dakota https://lpdaac.usgs.gov, Accessed date: 1
643   December 2019. Retrieved from
644   https://doi.org/10.5067/MEaSUREs/SRTM/SRTMUS1.003

645 Nefeslioglu, H. A., Gokceoglu, C., Sonmez, H., & Gorum, T. (2011). Medium-scale hazard
646   mapping for shallow landslide initiation: the Buyukkoy catchment area (Cayeli, Rize,
647   Turkey). *Landslides*, *8*(4), 459–483. https://doi.org/10.1007/s10346-011-0267-7

648 Owen, L. A., Kamp, U., Khattak, G. A., Harp, E. L., Keefer, D. K., & Bauer, M. A. (2008).
649   Landslides triggered by the 8 October 2005 Kashmir earthquake. *Geomorphology*, *94*(1–2),
650   1–9. https://doi.org/10.1016/j.geomorph.2007.04.007

651 Parker, R. N., Hancox, G. T., Petley, D. N., Massey, C. I., Densmore, A. L., & Rosser, N. J.
652   (2015). Spatial distributions of earthquake-induced landslides and hillslope preconditioning
653   in the northwest South Island, New Zealand. *Earth Surface Dynamics*, *3*(4), 501–525.
654   https://doi.org/10.5194/esurf-3-501-2015

655 Parker, Robert N., Densmore, A. L., Rosser, N. J., De Michele, M., Li, Y., Huang, R., … Petley,
656   D. N. (2011). Mass wasting triggered by the 2008 Wenchuan earthquake is greater than
657   orogenic growth. *Nature Geoscience*, *4*(7), 449–452. https://doi.org/10.1038/ngeo1154

658 Petley, D. (2012). Global patterns of loss of life from landslides. *Geology*, *40*(10), 927–930.
659   https://doi.org/10.1130/G33217.1

660 Petley, D. N., Hearn, G. J., Hart, A., Rosser, N. J., Dunning, S. A., Oven, K., & Mitchell, W. A.
661   (2007). Trends in landslide occurrence in Nepal. *Natural Hazards*, *43*(1), 23–44.
662   https://doi.org/10.1007/s11069-006-9100-3

663 Planet Team. (2017). Planet Application Program Interface: In Space for Life on Earth. San
664   Francisco, CA. https://api.planet.com.

665 Poesen, J. (2018). Soil erosion in the Anthropocene: Research needs. *Earth Surface Processes*
666   *and Landforms*, *43*(1), 64–84. https://doi.org/10.1002/esp.4250

667 Raja, N. B., Çiçek, I., Türkoğlu, N., Aydin, O., & Kawasaki, A. (2017). Landslide susceptibility
668   mapping of the Sera River Basin using logistic regression model. *Natural Hazards*, *85*(3),
669   1323–1346. https://doi.org/10.1007/s11069-016-2591-7

670 Reis, S., Nişanci, R., & Yomralioğlu, T. (2009). Designing and Developing a Province-Based
671   Spatial Database for the Analysis of Potential Environmental Issues in Trabzon, Turkey.
672   *Environmental Engineering Science*, *26*(1), 123–130. https://doi.org/10.1089/ees.2007.0158

673 Schmitt, R. G., Tanyas, H., Nowicki Jessee, M. A., Zhu, J., Biegel, K. M., Allstadt, K. E., …
674   Knudsen, K. L. (2017). An open repository of earthquake-triggered ground-failure
675   inventories. In *Data Series*. https://doi.org/10.3133/ds1064

676 Şekercioğlu, Ç. H., Anderson, S., Akçay, E., & Bilgin, R. (2011). Turkey's rich natural heritage
677   under assault. *Science*, *334*(6063), 1637–1639.

678 Şekercioğlu, Ç. H., Anderson, S., Akçay, E., Bilgin, R., Can, Ö. E., Semiz, G., … Nüzhet Dalfes,

679 H. (2011). Turkey's globally important biodiversity in crisis. *Biological Conservation*,

680 *144*(12), 2752–2769. https://doi.org/https://doi.org/10.1016/j.biocon.2011.06.025

681 Stark, C. P., & Guzzetti, F. (2009). Landslide rupture and the probability distribution of

682 mobilized debris volumes. *Journal of Geophysical Research: Earth Surface*, *114*(2), 1–16.

683 https://doi.org/10.1029/2008JF001008

684 Steffen, W., Broadgate, W., Deutsch, L., Gaffney, O., & Ludwig, C. (2015). The trajectory of the

685 Anthropocene: The Great Acceleration. *The Anthropocene Review*, *2*(1), 81–98.

686 https://doi.org/10.1177/2053019614564785

687 Steffen, W., Grinevald, J., Crutzen, P., & McNeill, John. (2011). The Anthropocene: conceptual

688 and historical perspectives. *Philosophical Transactions of the Royal Society A:*

689 *Mathematical, Physical and Engineering Sciences*, *369*(1938), 842–867.

690 https://doi.org/10.1098/rsta.2010.0327

691 Tang, C., Zhu, J., Qi, X., & Ding, J. (2011). Landslides induced by the Wenchuan earthquake

692 and the subsequent strong rainfall event: A case study in the Beichuan area of China.

693 *Engineering Geology*, *122*(1), 22–33.

694 https://doi.org/https://doi.org/10.1016/j.enggeo.2011.03.013

695 Tanyaş, H., Allstadt, K. E., & van Westen, C. J. (2018). An updated method for estimating

696 landslide-event magnitude. *Earth Surface Processes and Landforms*, *43*(9).

697 https://doi.org/10.1002/esp.4359

698 Tanyaş, H., van Westen, C. J., Allstadt, K. E., Anna Nowicki Jessee, M., Görüm, T., Jibson, R.

699 W., … Hovius, N. (2017). Presentation and Analysis of a Worldwide Database of

700 Earthquake-Induced Landslide Inventories. *Journal of Geophysical Research: Earth*

701 *Surface*, *122*(10). https://doi.org/10.1002/2017JF004236

702 Tanyaş, H., van Westen, C. J., Allstadt, K. E., & Jibson, R. W. (2019). Factors controlling

703 landslide frequency–area distributions. *Earth Surface Processes and Landforms*, *44*(4).

704 https://doi.org/10.1002/esp.4543

705 U.S. Geological Survey. (2017). Search Earthquake Catalog. Retrieved March 2, 2020, from

706   https://earthquake.usgs.gov/earthquakes/search/

707   Valdiya, K. S. (2014). Damming rivers in the tectonically resurgent Uttarakhand Himalaya.

708   *Current Science*, *106*(12), 1658–1668. Retrieved from

709   http://www.jstor.org/stable/24102998

710   Van Den Eeckhaut, M., Poesen, J., Govers, G., Verstraeten, G., & Demoulin, A. (2007).

711   Characteristics of the size distribution of recent and historical landslides in a populated hilly

712   region. *Earth and Planetary Science Letters*, *256*(3–4), 588–603.

713   https://doi.org/10.1016/j.epsl.2007.01.040

714   Vuillez, C., Tonini, M., Sudmeier-Rieux, K., Devkota, S., Derron, M.-H., & Jaboyedoff, M.

715   (2018). Land use changes, landslides and roads in the Phewa Watershed, Western Nepal

716   from 1979 to 2016. *Applied Geography*, *94*, 30–40.

717   https://doi.org/https://doi.org/10.1016/j.apgeog.2018.03.003

718   Waters, C. N., Zalasiewicz, J., Summerhayes, C., Barnosky, A. D., Poirier, C., Gałuszka, A., …

719   Wolfe, A. P. (2016). The Anthropocene is functionally and stratigraphically distinct from

720   the Holocene. *Science*, *351*(6269), aad2622. https://doi.org/10.1126/science.aad2622

721   WWF. (2020). Kamilet Havzası Bir Doğa Müzesi Olarak Saklanmalı. Retrieved from

722   https://www.wwf.org.tr/yayinlarimiz/basin_bultenleri/?10060/Kamilet-Havzasi-Bir-Doga-

723   Muzesi-Olarak-Saklanmali

724   Xu, C., Xu, X., Shyu, J. B. H., Zheng, W., & Min, W. (2014). Landslides triggered by the 22

725   July 2013 Minxian-Zhangxian, China, Mw 5.9 earthquake: Inventory compiling and spatial

726   distribution analysis. *Journal of Asian Earth Sciences*, *92*(July 2013), 125–142.

727   https://doi.org/10.1016/j.jseaes.2014.06.014

728   Yuksel, E., & Eminagaoglu, O. (2017). Flora Of The Kamilet Valley (Arhavi, Artvin, Turkey).

729   *International Journal of Ecosystems and Ecology Science-IJEES*, *7*(4), 905–914.

730

731

732

733